

## Estimation of uncertainty bounds for the future performance of a power plant

Odgaard, Peter Fogh; Stoustrup, Jakob

*Published in:*  
IEEE Transactions on Control Systems Technology

*DOI (link to publication from Publisher):*  
[10.1109/TCST.2008.922576](https://doi.org/10.1109/TCST.2008.922576)

*Publication date:*  
2009

*Document Version*  
Early version, also known as pre-print

[Link to publication from Aalborg University](#)

*Citation for published version (APA):*  
Odgaard, P. F., & Stoustrup, J. (2009). Estimation of uncertainty bounds for the future performance of a power plant. *IEEE Transactions on Control Systems Technology*, 17(1), 199 - 206.  
<https://doi.org/10.1109/TCST.2008.922576>

### General rights

Copyright and moral rights for the publications made accessible in the public portal are retained by the authors and/or other copyright owners and it is a condition of accessing publications that users recognise and abide by the legal requirements associated with these rights.

- Users may download and print one copy of any publication from the public portal for the purpose of private study or research.
- You may not further distribute the material or use it for any profit-making activity or commercial gain
- You may freely distribute the URL identifying the publication in the public portal -

### Take down policy

If you believe that this document breaches copyright please contact us at [vbn@aub.aau.dk](mailto:vbn@aub.aau.dk) providing details, and we will remove access to the work immediately and investigate your claim.

# Estimation of Uncertainty Bounds for the Future Performance of a Power Plant

Peter Fogh Odgaard, *Member, IEEE*, and Jakob Stoustrup, *Senior Member, IEEE*

**Abstract**—Prediction of the future performance of large-scale power plants can be very relevant for the operators of these plants, as the predictions can indicate possible problems or failures due to current operating conditions and/or future possible operating conditions. A problem in predicting the future performance of these plants is that available models of the plants are uncertain. In this brief, three schemes for predicting uncertain dynamical systems are presented. The schemes estimate upper and lower bounds on the system performance. Two of the schemes are statistically based, one only based on recent data and the other is based on operating points as well. The third proposed scheme uses dynamical models of the prediction uncertainties, like in  $H_\infty$ -control. The proposed schemes are subsequently applied to experimental data from a coal-fired power plant. Two sets of data from an actual power plant are used, one containing normal plant operation and in the second set, coal is accumulating in the coal mill due to an unbalance in the operating conditions. These tests showed that Schemes II and III did bound the real system performance, while Scheme I failed doing so. In addition, the plant was simulated operating under the same conditions with additional large disturbances. These simulations were used to investigate the robustness and conservatism of the proposed schemes. In this test, Schemes I and II failed, while Scheme III succeeded.

**Index Terms**—Dynamic prediction, power plants, statistical prediction, uncertain dynamical systems, uncertainty models.

## I. INTRODUCTION

PREDICTIONS of dynamical systems are important in a large number of applications and fields like: meteorology, biology, economics, physics, medicine, etc., see [1]–[4]. In control engineering prediction of dynamic systems represented by models is a key part of model predictive control, see [5]. Throughout this brief a model is used to represent the real system. The model is subsequently used to predict the future performance and behavior of the system. In most of the previous work on prediction of dynamic systems, the focus has been on adapting models to be representative at present as well. These models are subsequently used to predict the expected time series of the future behavior of the system, see [6] and [7]. Little focus has been on prediction of uncertain models where uncertainties and uncertain system conditions are taken into

account in the prediction. A proposed solution for predicting uncertain systems update the prediction model online, see, e.g., [6]. This is, however, not always a good solution to the problem, since a model identification will give new parameter values, but would not describe uncertainties due to model structures etc. Robust model predictive control is an exception, where worst case performances are included in the optimization, see [8]–[12]. These, however, do not directly give a prediction of the uncertainty of the system performance. Instead, they compute a control law which guarantees acceptable worst-case system performance.

In case of large-scale plants such as power plants, it is difficult to develop simple precise models, which do not deviate with time and thereby increasingly with the prediction horizon. During operation of these power plants, it would be helpful for the operator to use the predictor in a “what if” scenario, i.e. to know how the plant would perform in the future given certain operating conditions. The predictor should inform the operator if whether the variables of the plant are expected to stay within given intervals in the future or not. If the prediction indicates that these variables will drop out of the required intervals, the operators can take action accordingly. Hopefully this action is consequently taken earlier if these predictions are available, thereby preventing major plant failures or trips. Expected plant state performance are, in this case, not sufficient information for the operators, since these states would probably deviate from the expected values. Consequently, it would be helpful for the plant operator to have predictions of upper and lower bounds of the proper performance, given a certain probability, and these bounds shall consequently be contained in admissible plant variable intervals.

In a number of conference papers, the authors have proposed some schemes dealing with these prediction problems. In [13] and [14], two statistical methods are developed to estimate the uncertainty of the previous mentioned predictions. The first method uses statistics of recent windows of predictions, where a window is formed for each prediction horizon in question. The second method uses a bank of prediction error statistics depending on the operating point of the power plant, as well as on the prediction horizon. For many dynamical systems, the model uncertainties are deterministic rather than stochastic meaning it would be better to use a dynamical uncertainty model instead of a statistical one. In [15], the uncertainties were proposed computed using dynamical uncertainty models as used in  $H_\infty$ -theory, see [16]. The prediction uncertainty models are computed using output multiplicative uncertainty models.

In this brief, these three methods are applied to a coal-fired power plant, using data containing the problem due to the combination of high coal moisture content and high plant load. Two sets of experimental data are applied to these methods, one before the coal accumulation is occurring and one during the coal accumulation. These examples are used to evaluate how well

Manuscript received May 07, 2007; revised January 07, 2008. Manuscript received in final form March 13, 2008. First published May 14, 2008; current version published December 24, 2008. Recommended by Associate Editor A. Bazanella. This work was supported by the Danish Ministry of Science Technology and Innovation under Grant 2002-603/4001-93.

P. F. Odgaard was with Automation and Control, Department of Electronic Systems, Aalborg University, Fredrik Bajers Vej 7c, DK-9220 Aalborg East, Denmark. He is now with the KK-Electronic a/s, Jens Juuls Vej 40, DK-8260 Viby J, Denmark (e-mail: peodg@kk-electronic.com).

J. Stoustrup is with the Automation and Control, Department of Electronic Systems, Aalborg University, Fredrik Bajers Vej 7c, DK-9220 Aalborg East, Denmark (e-mail: jakob@es.aau.dk).

Color versions of one or more of the figures in this brief are available online at <http://ieeexplore.ieee.org>.

Digital Object Identifier 10.1109/TCST.2008.922576

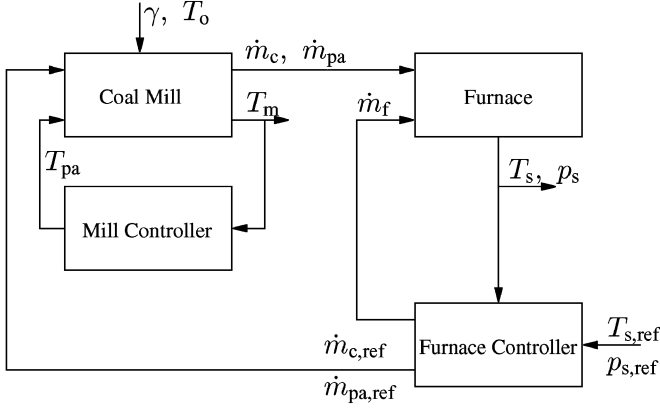


Fig. 1. Illustration of model structure.

the future plant performances are predicted in both faulty and fault-free cases. A reliable prediction is necessary if the operator should use these predictions of the future plant behavior and performance.

The degree of conservatism of these estimated uncertainty bounds are investigated by simulating the system behaviors as a response to realistic reference variations and disturbances.

In Section II, the coal-fired power plant which is the used example is shortly described. The proposed schemes for estimating these prediction uncertainty bounds are subsequently described starting with the statistically based schemes in Section III and the dynamical based one in Section IV. In Section V, these methods are applied to an example from a coal-fired power plant, where the coal flow into the furnace is limited due to a high coal moisture content and high plant load, resulting in a violation of an energy flow constraint in the coal mill. The degree of conservatism of the different estimated uncertainty bounds are inspected as well. In the end, a conclusion is drawn in Section VI.

## II. SYSTEM DESCRIPTION OF THE COAL-FIRED POWER PLANT

The proposed scheme is designed for predicting the performance of a coal-fired power plant, which is represented by an uncertain closed-loop model. The model used for predicting the plant performance is a combination of a furnace model found in [17] and [18], which is extended with a coal mill model, and controllers. An overview of the model structure can be seen in Fig. 1. The coal mill pulverizes and dries the coal dust, before it is blown into the furnace by the primary air flow.  $\dot{m}_c$  denotes the actual coal flow,  $\dot{m}_{c,ref}$  denotes the reference/requested coal flow,  $\dot{m}_{pa}$  denotes the actual primary air flow, and  $\dot{m}_{pa,ref}$  denotes the reference/requested primary air flow. Two disturbances to the coal mill are considered, these are the outside temperature,  $T_o$  and the coal moisture content  $\gamma$ . The temperature of the primary air flow is denoted  $T_{pa}$ . The primary air flow is used to dry and lift the coal dust into the furnace, and is used to keep the coal dust temperature  $T_m$  at 100 °C. In the furnace, the coal dust is burned and the hot flue gas is used to heat water to pressurized steam. Two crucial process variables, the steam temperature  $T_s$  and pressure  $p_s$  are used to control the plant, since references are given to those. This control results in coal flow and feed water flow  $\dot{m}_f$  requirements. The

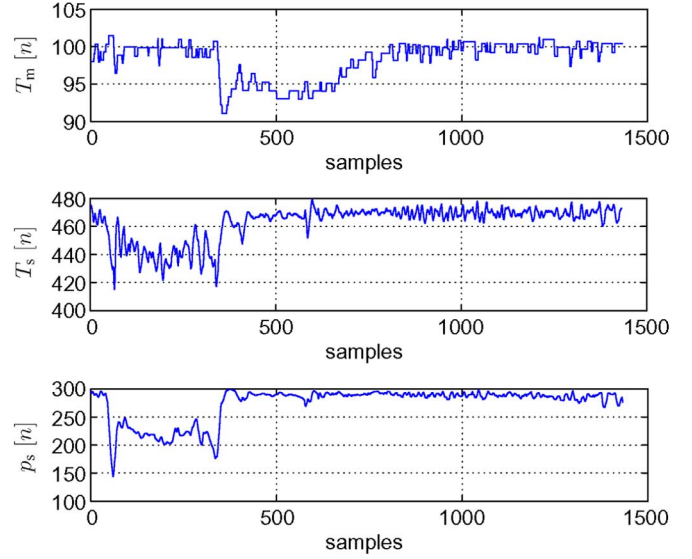


Fig. 2. Plots of the measurements of the mille temperature  $T_m$ , the steam temperature  $T_s$ , and the steam pressure  $p_s$ .

nonlinear plant model is subsequently linearized and reduced to a five-state linear model. The outputs of this linear model are coal mill temperature  $T_m$ , steam temperature  $T_s$ , and steam pressure  $p_s$ . Controlled inputs are the reference to steam temperature  $T_{s,ref}$  and the reference to steam pressure  $p_{s,ref}$ . A disturbance to the system, which is included in the model is the coal moisture  $\gamma$ , is estimated using the method presented in [19].

In this context, acceptable performance of the plant can be defined as selected plant variables being inside some specified bounds, meaning that the performance prediction is used to predict if the plant variable can be expected to be inside these specified bounds in the future. The nominal prediction model provides a less usable prediction of the future plant performance since uncertainties are not taken into account.

The experimental data used in this work contain (sampled with an interval of 60 s) a load change from a 85% load down to a 65% load, at sample 65, and up again to 85% load at sample 340. The measured outputs can be seen in Fig. 2. The moisture content, on the other hand, is increasing during the experiment from 14% to 15.5% at the time of the second load change. Consequently, not enough energy is available to heat and evaporate the moisture from the pulverized coal. This can be seen by the plot of  $T_m$ , in which decreases below the evaporation point of the moisture are seen. This is an example of a non-acceptable performance of the system. A consequence is that these wet coal particles are too heavy to be lifted up into the furnace by the primary air flow. Therefore, the coal particles are accumulated inside the coal mill. As a result, the master controller requests a higher coal flow. However, this leads to even more coal being accumulated in the coal mill instead of being blown into the furnace. In this case, the moisture content drops again, resulting in more coal being blown into the furnace than requested. Such a situation could result in an overheating of the plant. A safety stop is, consequently, necessary. Stops of the power plant are highly costly, so these should be avoided if possible, and prediction of future plant performance might help avoiding this.

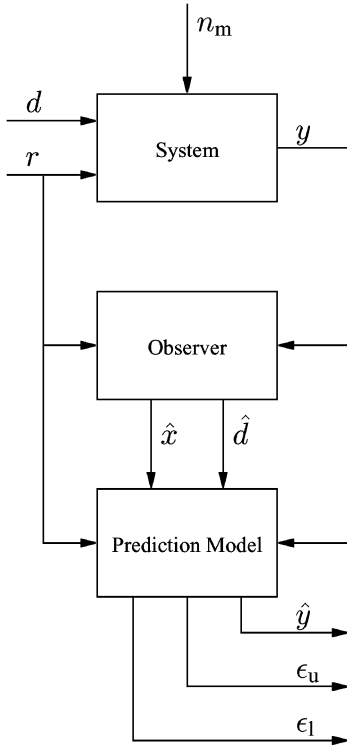


Fig. 3. Overview of the predictor structure, where the observer estimates the present states and in some cases the disturbances as well. The prediction model predicts the system behavior and uncertainties  $k$  steps into the future.

One should also notice that the references are known in advance since these are precomputed for guiding the load.

### III. STATISTICAL METHODS FOR ESTIMATING PREDICTION UNCERTAINTY BOUNDS

The two statistically-based predictors used in this brief are presented in [13] and [14]. These are based on the same general structure of the predictor, which is illustrated by Fig. 3, where the system inputs and outputs are used to estimate the present state values. These estimated values are fed to the predictor together with system inputs and outputs in order to predict the expected values as well as the uncertainty bounds.  $\hat{\mathbf{x}}[n]$  and  $\hat{\mathbf{d}}[n]$  denote the estimated state and disturbance vectors for the time instance  $n$ .  $\hat{\mathbf{y}}[n+k|n]$  is the vector of the predicted system output for the time  $n+k$  given  $n$ ,  $\epsilon_u[n+k|n]$  and  $\epsilon_l[n+k|n]$  denote, respectively, upper and lower bounds on system prediction for the time  $n+k$  given  $n$ . The observer and predictor (prediction model) will subsequently be described in more detail.

The closed-loop model is uncertain with respect to the real system. Consequently, an observer is introduced in order to estimate the value of the states at the sample time  $n$

$$\hat{\mathbf{x}}[n] = \mathbf{\Gamma}(\hat{\mathbf{x}}[n-1], \mathbf{r}[n], \mathbf{y}[n]) \quad (1)$$

where  $\mathbf{\Gamma}$  is an operator representing the observer, and  $\hat{\mathbf{x}}[n]$  is the estimated state vector at time  $n$ ,  $\mathbf{r}[n]$  is a vector of plant references, (the plant model describes a closed-loop system where a controller closes the loop), and  $\mathbf{y}[n]$  is a vector of plant outputs.

The estimated states can be used to predict the state and the output vector a number of samples into the future. It is assumed

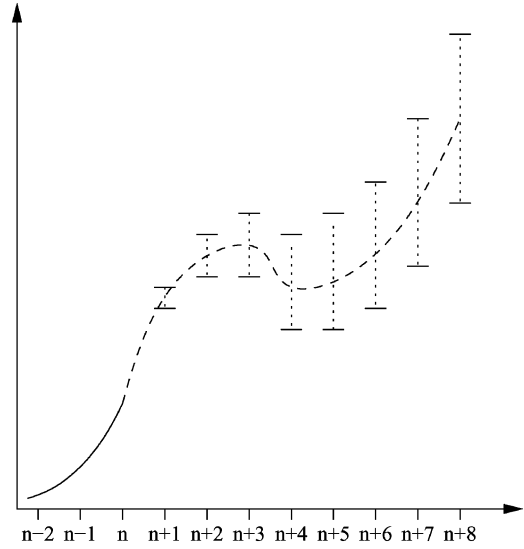


Fig. 4. Principle illustration of the uncertainty in the prediction. The uncertainty at each prediction step is increased as the number of prediction steps increases.

that the reference is partly known into the future due to a plan of the expected plant production, such as power plants, where the general power production is known one day ahead. The disturbance might be known up to time  $n$ , e.g., by estimation. Subsequently, these are denoted:  $\hat{\mathbf{r}}[n]$  and  $\hat{\mathbf{d}}[n]$ . The  $k$ -step predictor of the output  $\mathbf{y}[n+k|n]$  and states  $\mathbf{x}[n+k|n]$  are computed by

$$\mathbf{x}[n+1|n] = \mathbf{f}_m(\hat{\mathbf{x}}[n], \hat{\mathbf{r}}[n], \hat{\mathbf{d}}[n]) \quad (2)$$

where

$$\mathbf{x}[n+2|n] = \mathbf{f}_m(\mathbf{x}[n+1|n], \hat{\mathbf{r}}[n], \hat{\mathbf{d}}[n]) \quad (3)$$

continue this process until  $\mathbf{x}[n+k|n]$  is computed. Furthermore, compute

$$\hat{\mathbf{y}}[n+k|n] = \mathbf{g}_m(\mathbf{x}[n+k|n], \hat{\mathbf{r}}[n], \hat{\mathbf{d}}[n]). \quad (4)$$

Now, where the  $k$ -step predictor is defined, it is possible to define a  $k$ -step prediction error residual

$$\kappa[n+k|n] = \hat{\mathbf{y}}[n+k|n] - \mathbf{y}[n+k]. \quad (5)$$

This prediction error defined in (5) can of course only be computed earliest at sample  $n+k$ .

As previously stated, the model is assumed to be uncertain in relation to the real system. The variance of  $\kappa[n+N+1|n]$  is smaller than the variance of  $\kappa[n+N+2|n]$ . In other words, the prediction is expected to be more uncertain as the prediction horizon increases. This is illustrated by Fig. 4. The predicted system value is drawn with the dashed line, (from sample  $n+1$  to sample  $n+8$ ), the measured system output value is drawn with a solid line (sample  $n-2$  to  $n$ ). The uncertainties at the predicted values are marked by the vertical markings, with the small horizontal lines in the ends. The distance between these end markings represents the uncertainty for the specific predicted system value.

In the context mentioned in the introduction (see Section I), it is in the operator's interest to predict a region in which the system variables can be expected to be in, e.g., it is relevant for the operator to see how one can expect the performance of the plant to be given the prespecified conditions and references.

In this brief, two different statistically-based methods for predicting the uncertainty are compared. The first method computes means and variances of a given number of the most recent prediction errors at the prediction steps in question, see [13]. The advantage of this method is to be found if the model uncertainty is strongly time varying but independent of operating points. The second method uses a bank of precomputed mean and variance of prediction errors at different operating points (references, disturbances, etc.), see [14]. This method is preferable if model uncertainties are depending on the operating point and not strongly on time. It is as well possible to adapt the uncertainty model bank to present prediction errors.

#### A. Uncertainty Predictor—Method I

The uncertainty of the prediction can be represented in a number of ways. In this approach, the prediction error residuals are assumed to be a normal random process, with a specific variance and mean depending on the prediction step. The specific variance and mean will depend on the prediction step, depending on the vector of references  $\mathbf{r}$  and the vector of disturbances  $\mathbf{d}$ .  $\xi[n+k|n]$  is the predicted uncertainty at sample  $n+k$  given the estimate at  $n$

$$\xi[n+k|n] = \Phi(\sigma_{k,n}, \mu_{k,n}) \quad (6)$$

where  $\Phi$  is the normal distributed random process,  $\sigma_{k,n}$  is the variance of the  $k$ -step prediction error at sample  $n$ , and  $\mu_{k,n}$  is the mean of the  $k$ -step prediction error at sample  $n$ . These statistics are computed based on recorded prediction errors, where only the  $M$  most recent time samples are considered.

The variance  $\sigma_{k,n}$  can be computed as

$$\sigma_{k,n} = \text{var} \begin{pmatrix} \kappa[n-M+1|n-M+1-k] \\ \vdots \\ \kappa[n|n-k] \end{pmatrix}. \quad (7)$$

The mean  $\mu_{k,n}$  can be computed in a similar way

$$\mu_{k,n} = \text{mean} \begin{pmatrix} \kappa[n-M+1|n-M+1-k] \\ \vdots \\ \kappa[n|n-k] \end{pmatrix}. \quad (8)$$

These normal distributions can be used to compute uncertainty bounds ( $\epsilon_u$  and  $\epsilon_l$ ), on the prediction given a  $\eta$  confidence interval, i.e., the uncertainty bounds limit the possible system output values given probability of  $\eta$ .

For both statistical methods, the uncertainty prediction can be used to compute the upper and lower bounds of the prediction as

$$\epsilon_u[n+k|n] = \hat{\mathbf{y}}[n+k|n] + \xi[n+k|n] \quad (9)$$

$$\epsilon_l[n+k|n] = \hat{\mathbf{y}}[n+k|n] - \xi[n+k|n]. \quad (10)$$

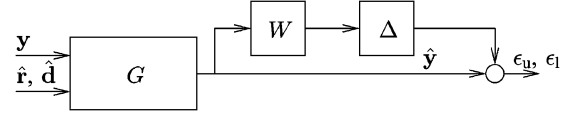


Fig. 5. Illustration of the nominal prediction model and multiplicative output prediction uncertainty model.

#### B. Uncertainty Predictor—Method II

In this approach, the uncertainty of the prediction is represented by a distribution depending on the references and possibly disturbances as well as the prediction length. This means that the mean and variance for different prediction steps are computed and used for different operating points in the reference and (disturbance).  $\xi[n+k|n]$  is the predicted uncertainty at sample  $n+k$  given estimate at  $n$ . Introducing dependency of the operating point leads to

$$\xi[n+k|n] = \Phi \left( \sigma_{\mathbf{r}[n+k], \mathbf{d}[n+k]}^k, \mu_{\mathbf{r}[n+k], \mathbf{d}[n+k]}^k \right) \quad (11)$$

where  $\Phi$  is the normal distributed random process,  $\sigma_{\mathbf{r}[n+k], \mathbf{d}[n+k]}^k$  is the variance of the  $k$ -step prediction error for reference at time  $n+k$  and disturbance at time  $n+k$ ,  $\mu_{\mathbf{r}[n+k], \mathbf{d}[n+k]}^k$  is the mean of the  $k$ -step prediction error for reference at time  $n+k$  and disturbance at time  $n+k$ .

*Uncertainty model parameter bank:* The statistics of prediction errors depend on operating points, which can be considered as uncertainty model parameters are stored in a data base, ordered accordingly to the depending variables, e.g.,  $\mathbf{r}[n+k]$  and  $\mathbf{d}[n+k]$  for  $k$ -step prediction. In this model parameter bank, model parameters are attached for every combination of depending variables. The simplest way to use these model parameters is to use the instance in the model bank which is closest to specified depending variables. However, linear interpolation between model elements are obvious to use, see [14].

### IV. DYNAMICAL METHODS FOR ESTIMATING PREDICTION UNCERTAINTY BOUNDS

The two previous methods were based on statistical methods, another way to predict the uncertainties is to use a method based on dynamical uncertainty models. The third method presented in this section is such a method.

#### A. Dynamical Uncertainty Model—Method III

The third approach proposed in this brief uses output multiplicative uncertainty models to model the prediction uncertainties from the nominal prediction model. The output multiplicative model is illustrated in Fig. 5, in which  $G$  represents the nominal prediction model fed with  $\mathbf{y}[n]$ ,  $\hat{\mathbf{r}}[N|n]$  and  $\hat{\mathbf{d}}[N|n]$ .  $\mathbf{W}[n]$  is the dynamical weighting function representing the bounding uncertainties and a scalar  $\Delta[n] \in \{-1 : 1\}$ . The output of the nominal prediction is  $\hat{\mathbf{y}}[N|n]$ , and the bounding uncertainty predictions are denoted  $\epsilon_u[N|n]$  and  $\epsilon_l[N|n]$  for the upper and lower bound, respectively. These bounds are defined as the maximal and minimal output of the uncertainty model.

These uncertainty predictions can be used to compute the upper and lower bounds of the prediction as in (9) and (10).  $\mathbf{W}[n]$  is defined as a filter bounding the frequency content of

the past prediction errors. Define a vector of the most recent predicted system values with specified prediction horizon  $k$  as

$$\hat{\mathbf{Y}}[q] = [\hat{y}[q+1|q] \quad \cdots \quad \hat{y}[q+k|q]] \quad (12)$$

for the time  $n$  the most recent vector is  $\hat{\mathbf{Y}}[n-k]$ . The corresponding vectors of measured system values can be defined as

$$\mathbf{Y}[q] = [y[q+1|q] \quad \cdots \quad y[q+k|q]]. \quad (13)$$

The vector of most recent prediction errors can be defined as

$$\mathbf{E}[q] = \mathbf{Y}[q] - \hat{\mathbf{Y}}[q]. \quad (14)$$

These pairs of relating  $\mathbf{E}[q]$  and  $\mathbf{Y}[q]$  vectors are subsequently grouped into different relevant points of operation given by references and disturbances. For each of these point-of-operation groups a filter  $\mathbf{W}[n]$  is computed as a filter bounding the difference between the nominal estimate and the measured data

$$\max_{\omega} (\text{FFT}(\mathbf{E}[q])), \quad \forall q \in Q_{r,d} \quad (15)$$

where  $\text{FFT}(\cdot)$  is the fast Fourier transform,  $Q_{r,d}$  is the set of pairs contained in the specified group of operating points.

In order to simplify the filter parameter identification the order and structure of  $\mathbf{W}[n]$  can be prespecified. In the example used in Section V, a first-order filter is used, and the parameters are found using MATLAB's *ident* toolbox.

To be certain that the bounds  $\epsilon$  covers the prediction uncertainties  $\Delta$  is set equal to 1. However, in practice this might be conservative, since  $\Delta = 1$  represents the worst-case model uncertainty seen in data. Instead,  $\Delta$  can be adapted to the present prediction uncertainty by

$$\Delta[n] = \frac{\|\text{FFT}(\mathbf{E}[n-k])\|}{\|\mathbf{W}[n]\|}. \quad (16)$$

The upper and lower bounds can subsequently be computed as in (9) and (10). In the case where  $\Delta$  is not corrected, (denoted in the sequel as "NC"), the bounds  $\epsilon$  is computed as

$$\epsilon[n] = \Delta \cdot \mathbf{W}[n] \cdot \hat{\mathbf{y}}[n] \quad (17)$$

and for the corrected  $\Delta$  (denoted as "C"), the bounds  $\epsilon$  is computed as

$$\epsilon[n] = \Delta[n] \cdot \mathbf{W}[n] \cdot \hat{\mathbf{y}}[n]. \quad (18)$$

In case this prediction scheme is used in as system with constraints, it should be remarked that non-feasible reference signals would raise problems for the nominal and uncertainty prediction. The non-feasible reference should be projected onto the feasible references.

## V. EXPERIMENTS WITH DATA FROM A COAL-FIRED POWER PLANT

The predictor of the uncertain system is applied to two sets of data from the coal-fired power plant presented in Section II. The measurements are sampled with intervals of 60 s. The first data set is during the low load, where the system performance

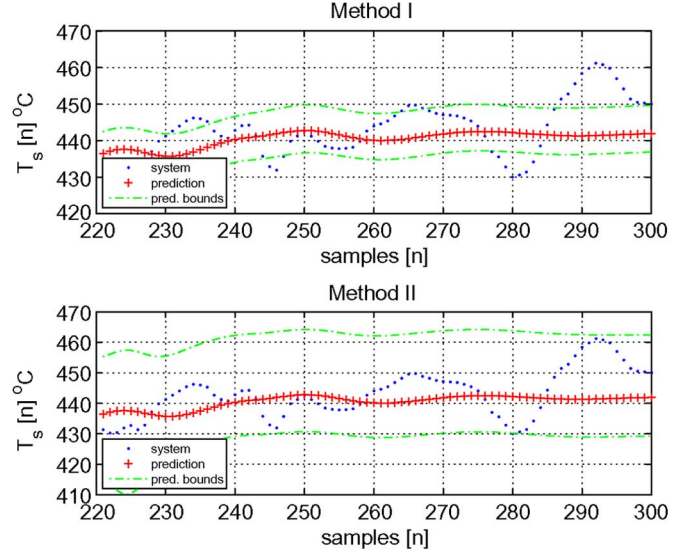


Fig. 6. Plot of prediction using the two statistical-based methods for  $T_s$ , predicted from sample 220 to sample 300. All prediction is performed from sample 220 and 80 samples into the future. The upper plot shows Method I and the lower plot shows Method II.

is predicted from sample no. 220 to 300. All prediction is performed from sample 220 and 80 samples into the future. At this time, accumulation of coal is not occurring. The second data set contains the problem of coal accumulation, where the system performance is predicted from sample 620 to sample 700. All prediction is performed from sample 621 and 80 samples into the future. Notice that in all plots the variables are predicted from the start value (sample 220 for Example I and 620 for Example II), and 1–80 steps into the future.

Mill and steam temperatures, as well as the steam pressure, are included in the prediction model, but in order to limit the number of plots of the predictions and measured plant performance, only the steam temperature,  $T_s$  plots are shown.

Notice that in the plotted predictions, see Fig. 6–13, the uncertainty bounds do not always contain the nominal prediction due to the introduction of the mean of the prediction error in the uncertainty model. This means that if a uncertainty model contains a mean value different from zero, the uncertainty bounds would be shifted relative to the nominal prediction.

### A. Statistically-Based Scheme Applied to the Data Set

In addition to the linear model described in Section II, an observer is used to estimate the state values. An optimal unknown input observer is used, see [20]. For the used uncertainty prediction methods a confidence interval at 90% is used.

The prediction of the steam temperature  $T_s$  can be seen in Fig. 6, in which the upper plot shows the predictions using Method I and the lower plot predictions using Method II. From Fig. 6, it can again be seen that the uncertainty bounds of Method II cover the measured system behavior while Method I does not cover all measurement points, (230–236, 246–247, 278–284, 287–300). From this set of experimental data and the prediction of system performance, it can be seen that Method

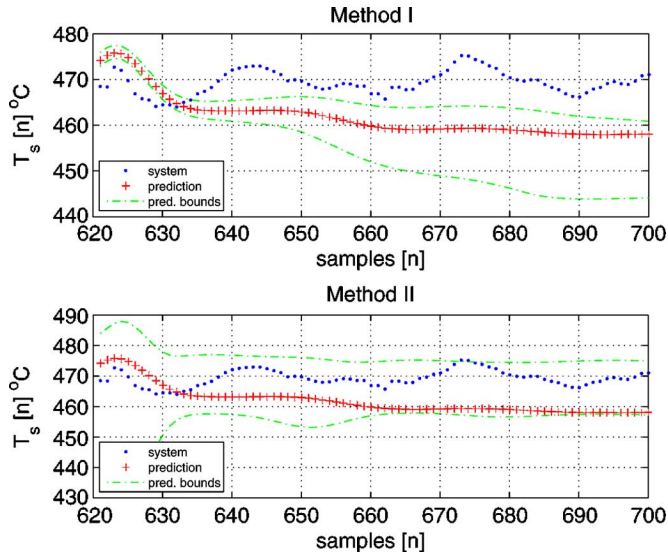


Fig. 7 Plot of predictions using the two statistical based methods for  $T_s$ , predicted from sample 620 to sample 700. All predictions are performed from sample 620 and 80 samples into the future. The upper plot shows Method I and the lower plot shows Method II.

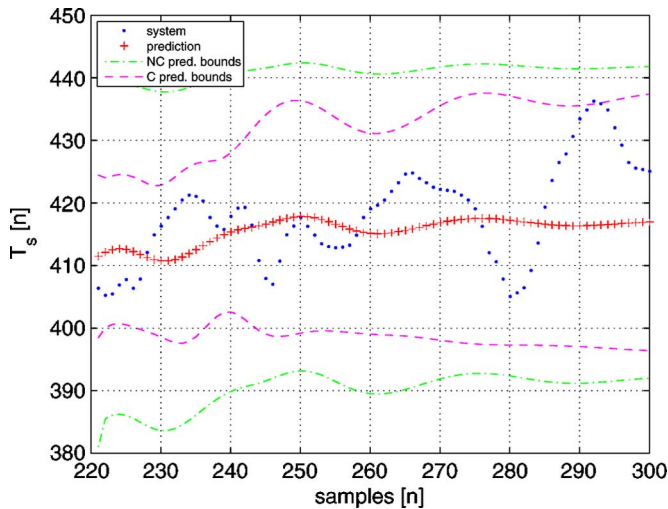


Fig. 8. Plot of  $T_s$  for Example 1. Both the non-corrected (NC) and corrected (C) uncertainty bounds contain the measured values.

I, using statistics of recent prediction errors has problems covering the system behavior. On the other hand Method II using statistics depending on operating points covers the system performance. This is a consequence of the model uncertainty depending more on the operating point than on time.

The attention is now put on the second set of measurements and predictions, from sample 620. Fig. 7 illustrates the predictions of  $T_s$ . It can be seen that only the uncertainty bounds of Method II covers the measured steam temperature  $T_s$ .

Using Method II, the uncertainty bounds obtained using Method II, provides the operator with knowledge on the future performance of the system, given the specified operating conditions can use these uncertainty predictions. These proposed schemes for predicting uncertain dynamical systems can be used in other power plant cases, e.g., start-up of the plant where specific state values shall be reached in a given time, in this case

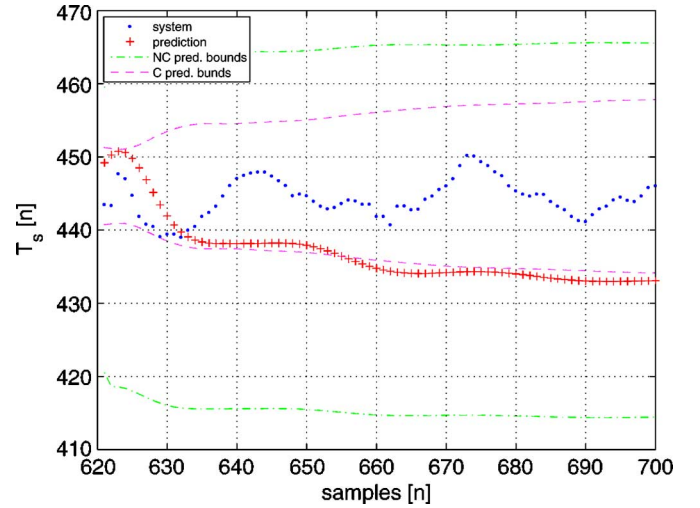


Fig. 9. Plot of  $T_s$  for Example 2. Both the non-corrected (NC) and corrected (C) uncertainty bounds contain the measured values.

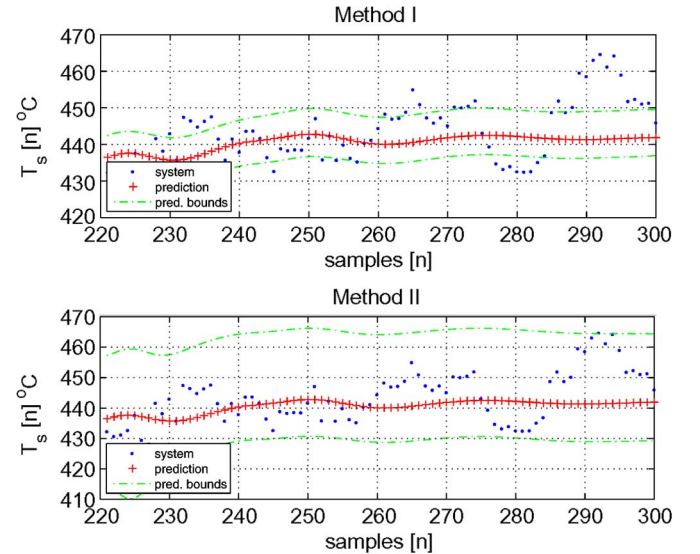


Fig. 10. Plot of predictions using the two statistical based methods for  $T_s$ , predicted from sample 220 to sample 300. All predictions are performed from sample 220 and 80 samples into the future (Example 1). The upper plot shows Method I and the lower plot shows Method II.

the operator can use these uncertainty predictions to see how start-up is proceeding and eventually take action if required.

### B. Dynamical-Based Scheme Applied to the Data Set

These experiments are used to validate that the dynamical uncertainty predictor can estimate the measured system variables during different plant conditions. The predictor of the uncertain system is applied to the same two sets of data as the statistically based schemes were. Again, only the steam temperature is shown.

The prediction for Example 1 can be seen in Fig. 8, and the plot of Example II are plotted in Fig. 9. In each of the plots both the non-corrected prediction bounds and the corrected prediction bounds are plotted.

From these, it can be seen that the computed uncertainty bounds cover all the measured variables, both in the corrected

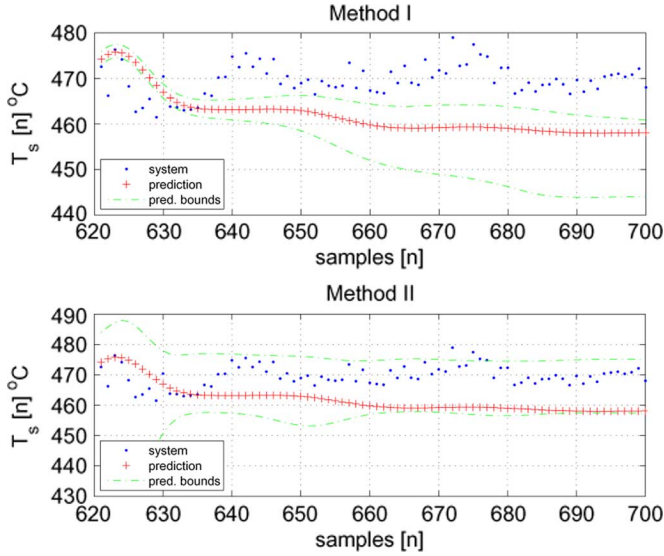


Fig. 11. Plot of predictions using the two statistical based methods for  $T_s$ , predicted from sample 620 to sample 700. All predictions are performed from sample 620 and 80 samples into the future (Example 2). The upper plot shows Method I and the lower plot shows Method II.

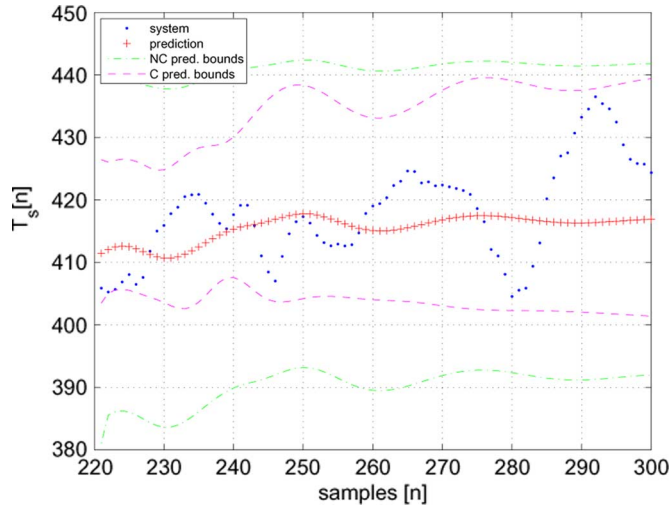


Fig. 12. Plot of  $T_s$  for Example 1. Both the non-corrected (NC) and corrected (C) uncertainty bounds contain the measured values.

and non-corrected cases and for both examples. However, the nominal prediction is not covered for all samples due to low frequently modeling errors. The corrected uncertainty prediction bounds narrow the uncertainty region as expected, and as mentioned previously, still contain the measured values.

### C. Experiments to Assess Conservatism

In order to test the conservatism of the estimated uncertainty bounds, the experiments are simulated with highly increased disturbances and measurement noises. An extended nonlinear simulation model of the power plant is used, see [21]. These sets of simulated plant data are subsequently used in the same manner as the experimental data was previously. However, in

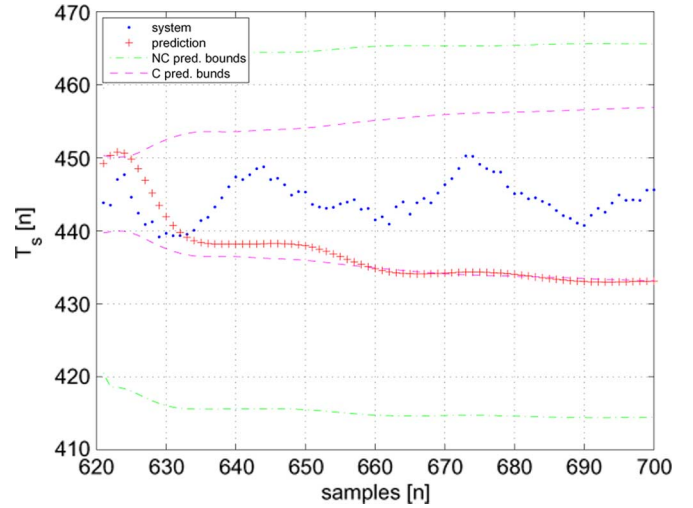


Fig. 13. Plot of  $T_s$  for Example 2. Both the non-corrected (NC) and corrected (C) uncertainty bounds contain the measured values.

order to limit the number of repeated plots only the steam temperatures  $T_s$  are plotted.

In Fig. 10, Method I is applied to the statistically-based schemes. From Fig. 10, it can be seen that the prediction uncertainty bounds do not cover the simulated output. Fig. 11 shows the statistically-based schemes for Case II, in which the first approach does not cover the simulated variable, while Approach II bounds the simulated variable, but the variable varies close to both the upper and lower bounds, meaning that it does not seem very conservative. However, since the second statistic approach did not cover  $T_s$  for the first example as well, it can be concluded that the statistical method cannot cover these additional disturbances. In Figs. 12 and 13, the dynamical-based uncertainty estimation scheme is applied to the two examples. In both cases,  $T_s$  stays inside the uncertainty bounds, but do get close to these, meaning that the dynamical-based scheme is both robust towards these disturbances and as well not too conservative. The same is valid for the predictions of the other variables not presented here.

*Summary on experiments:* From the experiments with the three proposed schemes it can be seen that the uncertainties in this case depends on the reference values as well as on the disturbances. If the uncertainty models are independent of these, the uncertainty bounds will only cover the system performance if these bounds are computed very conservatively. Robustness as well as the degree of conservatism of the computed uncertainty bounds were investigated using additional disturbances and noises in a simulation model representing the experiments. From these simulations, it can be concluded that the two statistically-based schemes were not robust towards the specific disturbances. The dynamical-based scheme did, however, cover the system variable in presence of these large disturbances. In addition it could also be seen that the dynamical computed uncertainty bounds were close to the simulated system variables meaning that the scheme on the other hand was not too conservative. All in all, these experiments indicate

that the proposed dynamical uncertainty bounds scheme has potential for prediction of the power plant performance.

## VI. CONCLUSION

In this brief, three schemes for predicting performance of a coal-fired power plant, represented by an uncertain dynamical systems, are presented. The schemes estimate upper and lower bounds on the system performance. Two of the schemes were statistically based, one only based on recent data and the other is based on operating points as well. The third proposed scheme uses dynamical models of the prediction uncertainties, like in  $H_\infty$ -control. The proposed schemes are subsequently applied to experimental data from the coal-fired power plant in mind. Two sets of data from an actual power plant are used, one containing normal plant operation and in the second set coal is accumulating in the coal mill due to an unbalanced combination of the operating conditions. These tests showed that Methods II and III did bound the real system performance, while Method I failed doing so. In addition, the plant was simulated operating under the same conditions with additional large disturbances. These simulations were used to investigate the robustness and conservatism of the proposed schemes. In this test, Methods I and II failed, while Method III succeeded. This means that the dynamical uncertainty prediction scheme can be used to predict the plant performance.

## REFERENCES

- [1] J. W. Hansen, A. Potgieter, and M. K. Tippett, "Using a general circulation model to forecast regional wheat yields in Northeast Australia," *Agricultural Forest Meteorology*, vol. 127, pp. 77–92, Dec. 2004.
- [2] A. M. Feigin, Y. I. Molkov, D. N. Muhkin, and E. M. Loskutov, "Prognosis of qualitative behavior of a dynamic system by the observed chaotic time series," *Radiophys. Quantum Electron.*, vol. 44, pp. 376–398, May–Jun. 2001.
- [3] L. Y. Bukharbaeva, I. R. Rakhmatullina, and M. Tanyukevich, "Dynamic system simulation for prediction of the number of patients with malignant tumors in various clinical groups and assessment of the demand for financial resources," *Biomed. Eng.*, vol. 38, pp. 86–90, Feb. 2004.
- [4] C. Viboud, P.-Y. Boëlle, F. Carrat, A.-J. Valleron, and A. Flahault, "Prediction of the spread of influenza epidemics by the method of analogues," *Amer. J. Epidemiology*, vol. 158, pp. 996–1006, November 2003.
- [5] E. F. Camacho and C. Bordons, *Model Predictive Control*, 2nd ed. New York: Springer, 2002.
- [6] M. Milanese and C. Novara, "Set membership prediction of nonlinear time series," *IEEE Trans. Autom. Control*, vol. 50, no. 11, pp. 1655–1669, Nov. 2005.
- [7] A. Naess, "Prediction of extreme response of nonlinear structures by extended stochastic linearization," *Probabilistic Eng. Mech.*, vol. 10, pp. 153–160, Jul. 1995.
- [8] Y. J. Wang and J. B. Rawlings, "A new robust model predictive control Method I: Theory and computation," *J. Process Control*, vol. 14, pp. 231–247, Mar. 2004.
- [9] Y. J. Wang and J. B. Rawlings, "A new robust model predictive control Method II: Examples," *J. Process Control*, vol. 14, pp. 249–262, Mar. 2004.
- [10] G. Pannocchia, "Robust model predictive control with guaranteed set-point tracking," *J. Process Control*, vol. 14, pp. 927–937, Aug. 2004.
- [11] M. Diehl and Björnver, "Robust dynamic programming for min-max model predictive control of constrained uncertain systems," *IEEE Trans. Autom. Control*, vol. 49, pp. 2253–2257, Dec. 2004.
- [12] L.-S. Hu, B. Huang, and Y.-Y. Cao, "Robust digital model predictive control for linear uncertain systems with saturation," *IEEE Trans. Autom. Control*, vol. 49, no. 5, pp. 792–796, May 2004.
- [13] P. Odgaard, J. Stoustrup, and B. Mataji, "Prediction of lacking control power in power plants using statistical models," in *Proc. Euro. Control Conf.*, Kos, Greece, Jul. 2007, pp. 4679–4684, 2007.
- [14] P. Odgaard, J. Stoustrup, and B. Mataji, "Using reference trajectories to predicted uncertain systems: Exemplified on a power plant," in *Proc. Amer. Control Conf.*, New York City, Jul. 2007, pp. 6055–6060, 2007.
- [15] P. Odgaard, J. Stoustrup, and B. Mataji, "Using dynamical uncertainty models estimating uncertainty bounds on power plant performance prediction," in *Proc. Euro. Control Conf.*, Kos, Greece, Jul. 2007, pp. 4728–4733, 2007.
- [16] K. Zhou, J. C. Doyle, and K. Glover, *Robust and Optimal Control*, 1st ed. Englewood Cliffs, NJ: Prentice-Hall, 1996.
- [17] J. Bendtsen, J. Stoustrup, and K. Trangbaek, "Multi-dimensional gain scheduling with application to power plant control," in *Proc. 42nd IEEE Conf. Dec. Control*, Maui, HI, Dec. 2003, vol. 6, pp. 6553–6558.
- [18] J. Bendtsen, J. Stoustrup, and K. Trangbaek, "Bumpless transfer between advanced controllers with applications to power plant control," in *Proc. 42nd IEEE Conf. Dec. Control*, Maui, HI, Dec. 2003, vol. 3, pp. 2059–2064.
- [19] P. Odgaard and B. Mataji, "Estimation of moisture content in coal in coal mills," presented at the IFAC Symp. Power Plants Power Syst., Kananskis, AB, Canada, Jun. 2006.
- [20] J. Chen and R. J. Patton, *Robust Model-Based Fault Diagnosis for Dynamic Systems*, 1st ed. Norwell, MA: Kluwer Academic, 1999.
- [21] P. Odgaard, J. Stoustrup, and B. Mataji, "Preventing performance drops of coal mills due to high moisture content," in *Proc. Euro. Control Conf.*, Kos, Greece, Jul. 2007, pp. 4734–4739, 2007.